OsteoArthritis and Cartilage (2006) **14,** 554–560

doi:10.1016/j.joca.2005.12.006

Osteoarthritis and Cartilage

International Cartilage Repair Society

OARSI OSTEOARTHRITIS RESEARCH SOCIETY INTERNATIONAL

A composition-based cartilage model for the assessment of compositional changes during cartilage damage and adaptation

Dr. W. Wilson Ph.D., Dr. J. M. Huyghe Ph.D. and Dr. C. C. van Donkelaar Ph.D.*
Department of Biomedical Engineering, Eindhoven University of Technology, P.O. Box 513, 5600 MB Eindhoven, The Netherlands

Summary

Objective: The composition of articular cartilage changes with progression of osteoarthritis. Since compositional changes are associated with changes in the mechanical properties of the tissue, they are relevant for understanding how mechanical loading induces progression. The objective of this study is to present a computational model of articular cartilage which enables to study the interaction between composition and mechanics.

Methods: Our previously developed fibril-reinforced poroviscoelastic swelling model for articular cartilage was combined with our tissue composition-based model. In the combined model both the depth- and strain-dependencies of the permeability are governed by tissue composition. All local mechanical properties in the combined model are directly related to the local composition of the tissue, i.e., to the local amounts of proteoglycans and collagens and to tissue anisotropy.

Results: Solely based on the composition of the cartilage, we were able to predict the equilibrium and transient response of articular cartilage during confined compression, unconfined compression, indentation and two different 1D-swelling tests, simultaneously.

Conclusion: Since both the static and the time-dependent mechanical properties have now become fully dependent on tissue composition, the model allows assessing the mechanical consequences of compositional changes seen during osteoarthritis without further assumptions. This is a major step forward in quantitative evaluations of osteoarthritis progression.

Key words: Cartilage, Permeability, Intra-fibrillar, Depth-dependent, Finite element analysis.

Introduction

Articular cartilage covers the articulating ends of diarthrodial joints. It serves to allow almost frictionless motion, distribute the loads over a large contact area, and dissipate the energy associated with dynamic loads. Osteoarthritis which involves degeneration of the articular cartilage is the most common cause of disability in the elderly. During this disease both the structure and composition of articular cartilage change. Computer models have been successful in predicting the initial changes that occur during cartilage damage initiation[1–3]. To study the influence of these changes on the progression of cartilage damage, which is mostly induced by excessive loading at high loading rates, a model is needed that can take into account local changes in tissue constitution as well as the transient mechanical tissue behavior. Therefore the goal of this study was to develop a model for articular cartilage in which all local material properties that determine the equilibrium and the transient behavior are the direct consequence of the local composition of the tissue. Such a model enables us to study the influence of local changes in composition that occur during cartilage degeneration and adaptation.

We have recently developed a model in which the equilibrium behavior of articular cartilage is the direct result of its local composition[4]. With this model we were able to explain the depth- and strain-dependent equilibrium behavior of articular cartilage during confined compression. To be able to account for the transient behavior as well, the model must be extended to include viscoelastic behavior. This essential model extension requires validation with experimental data from literature.

Two distinct mechanisms are responsible for the viscoelastic behavior of articular cartilage[5–7]: the frictional drag force of interstitial fluid flow through the porous solid matrix (i.e., the flow-dependent mechanism) and the time-dependent deformability of the solid matrix (i.e., the flow-independent mechanism). Fluid movement in loaded cartilage is governed by the hydraulic permeability of the solid matrix. It was shown that the negative fixed charge density of the proteoglycans limits fluid flow and thereby affects the permeability of the tissue[8–11]. The permeability is also highly dependent on pore sizes in the extracellular matrix[10–14]. When the tissue is deformed the fixed charge density and pore sizes change[8,10,11,14,15]. Hence, the permeability of cartilage is strain-dependent. It has also been shown that the permeability in articular cartilage is depth-dependent[16,17].

Several empirical equations for deformation-dependent permeability of cartilage have been proposed[13,15,18,19]. In these empirical equations the permeability is based on the changes in fluid content of the tissue. However, not all the fluid is able to flow out freely. Part of the water in the tissue

*Address correspondence and reprint requests to: Dr Corrinus C. van Donkelaar, Ph.D., Department of Biomedical Engineering, WH 4.118, Eindhoven University of Technology, P.O. Box 513, 5600 MB Eindhoven, The Netherlands. Tel: 31-40-247-3135; Fax: 31-40-244-7355; E-mail: c.c.v.donkelaar@tue.nl
Received 4 October 2005; revision accepted 20 December 2005.

is absorbed by the collagen fibrils[20–23]. It has been shown that the amount of intra-fibrillar water depends on the osmotic pressure in the tissue[23]. As the osmotic pressure is highly dependent on volumetric strain, this introduces an additional strain-dependency of the permeability.

We hypothesize that if the properties of the constituents of articular cartilage are chosen correctly, the appropriate global and depth-dependent cartilage behavior, including permeability, results from the composition of the tissue.

To asses this hypothesis a relation between permeability and tissue composition is derived. This relation together with a new viscoelastic law for the collagen fibrils will be implemented in the model of Wilson *et al.*[4]. To determine the unknown material parameters and to validate the model, the model was fitted to confined compression, unconfined compression and indentation data of DiSilvestro and Suh[24] and to 1D-swelling data of Wilson *et al.*[4] and Eisenberg and Grodzinsky[25].

Methods

MODEL

In the fibril-reinforced poroviscoelastic swelling theory[4,26], articular cartilage is assumed as biphasic, consisting of a porous solid matrix saturated with water. The porous solid matrix consists of a swelling nonfibrillar part which contains mainly proteoglycans, and a fibrillar part representing the collagen network. According to Wilson *et al.*[4] the total tissue stress is given by

$$\boldsymbol{\sigma}_{\text{tot}} = -\mu_{\text{f}}\mathbf{I} + n_{\text{s,0}}\left(\left(1 - \sum_{i=1}^{\text{totf}} \rho_{\text{c}}^{i}\right)\boldsymbol{\sigma}_{\text{nf}} + \sum_{i=1}^{\text{totf}} \rho_{\text{c}}^{i}\boldsymbol{\sigma}_{\text{f}}^{i}\right) - \Delta\pi\mathbf{I}, \quad (1)$$

where μ_{f} is the water chemical potential, $\mathbf{I}$ the unit tensor, $\Delta\pi$ the osmotic pressure gradient, $n_{\text{s,0}}$ the initial solid volume (in the unloaded and nonswollen state), $\boldsymbol{\sigma}_{\text{nf}}$ the stress in the nonfibrillar matrix, $\boldsymbol{\sigma}_{\text{f}}^{i}$ the fibril stress in the ith fibril with respect to the global coordinate system, totf the total number of fibril compartments included, and ρ_{c}^{i} the volume fraction of the collagen fibrils in the ith direction with respect to the total solid volume.

Fibrillar part

The fibril stress tensor is given by[4]

$$\boldsymbol{\sigma}_{\text{f}} = \frac{\lambda}{J} P_{\text{f}} \vec{e}_{\text{f}} \vec{e}_{\text{f}}, \quad (2)$$

where J is the determinant of the deformation tensor $\mathbf{F}$, λ the elongation of the fibril, P_{f} the first Piola–Kirchhoff fibril stress, and $\vec{e}_{\text{f}}$ the current fibril direction. In Wilson *et al.*[26] the viscoelastic behavior of the collagen fibrils was represented by a linear spring S_1, parallel to a nonlinear spring S_2 in series with a linear dashpot with dashpot constant η (Fig. 1). Hence, the equilibrium stiffness of the collagen fibrils was assumed to be strain-independent. However, Charlebois *et al.*[27] have shown that the equilibrium stiffness of the collagen fibrils is strain-dependent. Therefore, the mechanical behaviors of springs S_1 and S_2 were replaced by the two-parameter exponential stress–strain relationships[28–31]

$$\begin{array}{ll} P_1 = E_1\left(e^{k_1\varepsilon_{\text{f}}} - 1\right) & \text{for } \varepsilon_{\text{f}} > 0 \\ P_1 = 0 & \text{for } \varepsilon_{\text{f}} \le 0 \end{array} \quad (3)$$

and

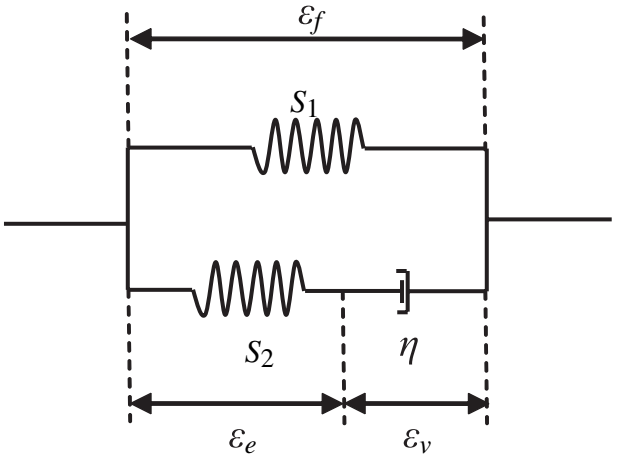

Fig. 1. Schematic model for a viscoelastic collagen fibril (ε_{f} is the total fibril strain, ε_{v} the dashpot strain and ε_{e} the strain in spring S_2).

$$\begin{array}{ll} P_2 = E_2\left(e^{k_2\varepsilon_{\text{e}}} - 1\right) & \text{for } \varepsilon_{\text{e}} > 0 \\ P_2 = 0 & \text{for } \varepsilon_{\text{e}} \le 0 \end{array}, \quad (4)$$

respectively, with E_1, E_2, k_1 and k_2 positive material constants, ε_{f} the total fibril strain, and ε_{e} the strain in spring S_2. Since the strains in the upper and lower part of the spring system in Fig. 1 are the same, the total fibril stress is given by

$$P_{\text{f}} = P_1 + P_2. \quad (5)$$

The derivation of P_2 as a function of the fibril strain ε_{f} is given in Appendix A.

As discussed in Wilson *et al.*[26] the fibril structure was implemented as two primary and seven secondary fibril directions. The density of each fibril with respect to the total collagen density is given by

$$\begin{array}{ll} \rho_{\text{c}} = \rho_{\text{c,tot}}\dfrac{C}{2C+7} & \text{for the primary fibrils} \\ \rho_{\text{c}} = \rho_{\text{c,tot}}\dfrac{1}{2C+7} & \text{for the secondary fibrils} \end{array}, \quad (6)$$

with C a positive constant greater than 1. For the determination of the fibril strains and directions, the reader is referred to Wilson *et al.*[26,32].

Nonfibrillar part

Although the solid material itself is virtually incompressible due to its porous structure, the entire solid matrix is compressible. For a solid fraction of 1 there are no pores, hence the entire matrix has become incompressible. As the solid fraction approaches 0 the volume fraction of the pores approaches 1. Because the pores themselves are fully compressible the entire solid matrix is also fully compressible. Based on the assumption that the solid matrix becomes incompressible when the solid fraction approaches 1 and becomes fully compressible when the solid fraction approaches 0, the stress in the nonfibrillar solid matrix is given by following modified Neo-Hookean law[4],

$$\boldsymbol{\sigma}_{\text{nf}} = -\frac{1}{6}\frac{\log(J)}{J}G_{\text{m}}\mathbf{I}\left[-1 + \frac{3(J+n_{\text{s,0}})}{(-J+n_{\text{s,0}})} + \frac{3\log(J)Jn_{\text{s,0}}}{(-J+n_{\text{s,0}})^2}\right] + \frac{G_{\text{m}}}{J}\left(\mathbf{F}\cdot\mathbf{F}^{\text{T}} - J^{2/3}\mathbf{I}\right), \quad (7)$$

where G_{m} is the shear modulus.

Osmotic swelling

For the swelling behavior the biphasic swelling theory[26,33] was used. This theory is based on the hypothesis that electrolyte flux can be neglected in mechanical studies of charged materials[34]. This means the ion concentrations can always be assumed in equilibrium.

When the distinction between extra- and intra-fibrillar water is taken into account, the effective fixed charge density should be expressed as mEq fixed charges per ml extra-fibrillar water and not based on the total fluid content as is usually done. The osmotic pressure gradient $\Delta\pi$ is then given by[4]

$$\Delta\pi = \phi_{\text{int}} \text{RT} \sqrt{c_{\text{F,exf}}^2 + 4\frac{\left(\gamma_{\text{ext}}^{\pm}\right)^2}{\left(\gamma_{\text{int}}^{\pm}\right)^2} c_{\text{ext}}^2} - 2\phi_{\text{ext}} \text{RT} c_{\text{ext}}. \tag{8}$$

where the fixed charge density based on the extra-fibrillar fluid fraction $c_{\text{F,exf}}$, is given by

$$c_{\text{F,exf}} = \frac{n_{\text{f}} c_{\text{F}}}{n_{\text{exf}}}, \tag{9}$$

with n_{f} the total fluid fraction, n_{exf} the extra-fibrillar fluid fraction and c_{F} the normal fixed charge density in mEq per ml total fluid. For more details about determining the extra-fibrillar fluid fraction the reader is referred to Wilson *et al.*[4]. The osmotic (ϕ_α) and activity coefficients (γ_α) were implemented as proposed by Huyghe *et al.*[35]. The external salt concentration (c_{ext}) was 0.15 M, the temperature (T) 293 K and the gas constant (R) 8.3145 $\times$ 10^{-3} N m/mmol K.

Permeability

In Wilson *et al.*[26,32] the permeability (k) was assumed to be strain-dependent, and given by[36]

$$k = k_0 \left(\frac{1+e}{1+e_0}\right)^M = k_0 \left(\frac{1-n_{\text{f,0}}}{1-n_{\text{f}}}\right)^M, \tag{10}$$

where k_0 is the initial permeability, M a positive constant, and e and e_0 the current and initial void ratios, respectively, and n_{f} and $n_{\text{f,0}}$ the current and initial fluid fractions, respectively. When accounting for the fact that only the extra-fibrillar fluid can flow out of the tissue, this becomes

$$k = k_0 \left(\frac{1-n_{\text{exf,0}}}{1-n_{\text{exf}}}\right)^M. \tag{11}$$

Based on the assumption that the depth- and strain-dependent permeabilities are governed by the same mechanism, the initial extra-fibrillar fluid fraction $n_{\text{exf,0}}$ is replaced by a reference value c_{ref} that is constant over the depth of the tissue

$$k = k_0 \left(\frac{1-c_{\text{ref}}}{1-n_{\text{exf}}}\right)^M = \alpha (1-n_{\text{exf}})^{-M}, \tag{12}$$

with α a positive material constant. Hence, the permeability is only a function of the current extra-fibrillar fluid fraction.

Composition

The fluid fraction, collagen fraction and fixed charge density distributions as a function of the normalized depth z^* were taken the same as in Wilson *et al.*[4].

$$n_{\text{f}} = 0.9 - 0.2z^*, \tag{13}$$

$$n_{\text{coll}} = 1.4(z^*)^2 - 1.1z^* + 0.59, \tag{14}$$

$$c_{\text{F}} = -0.10(z^*)^2 + 0.24z^* + 0.035, \tag{15}$$

where n_{f} is the total fluid volume fraction, n_{coll} the collagen density per solid volume, and c_{F} the fixed charge density in mEq/ml water.

The model was implemented in ABAQUS v6.5-1 (Hibbitt, Karlsson & Sorensen, Inc., Pawtucket, RI, USA). For more details about this model see Wilson *et al.*[4,26,32].

DETERMINATION OF UNKNOWN MATERIAL PROPERTIES

Based on Wilson *et al.*[26] we used $C = 3$ [Eq. (6)]. The factor M was directly determined by fitting Eq. (12) to the depth-dependent permeability as measured by Maroudas[17]. The shear modulus G_{m} was determined by fitting the model to the 1D-swelling data from Eisenberg and Grodzinsky[25]. The remaining unknown material parameters E_1, E_2, k_1, k_2, η_0 and α were determined by fitting them to the confined compression, unconfined compression and indentation data of DiSilvestro and Suh[24] and the 1D-swelling data of Wilson *et al.*[4]. The fitting procedures were the same as used in Wilson *et al.*[4,26,32]. For the confined compression, unconfined compression and indentation tests the same meshes and boundary conditions were used as in Wilson *et al.*[26]. For the 1D-swelling tests the same meshes and boundary conditions were used as in Wilson *et al.*[4]. The experiments are briefly described below.

In the 1D-swelling test of Wilson *et al.*[4] the free swelling strains of articular cartilage were measured as a function of the external salt concentration at 0.00, 0.07, 0.15, 0.30, 0.67, 1 and 2 M NaCl. The swelling strain was assumed to be 0 at an external salt concentration of 2 M NaCl. These tests were performed on cartilage from calf tibia plateaus with an average thickness of 1.03 mm.

In the 1D-swelling experiments of Eisenberg and Grodzinsky[25] cartilage plugs with a radius of 3.2 mm were axially compressed by 15% in a confined compression setup. After full relaxation, the external salt concentration was decreased to 0.0001 M. After equilibrium the salt concentration was repeatedly increased with 0.05 M until an external salt concentration of 2 M was reached. During this process the height of the sample was held constant, while the axial reaction forces were computed. The used samples were taken from the patellae-femoral groove of mature 1–2-year-old cattle.

During the confined compression, unconfined compression and indentation test of DiSilvestro and Suh[24], cartilage plugs with a radius of 1.5 mm and an average thickness of 1.281 mm were compressed with 10% either a flat platen (confined and unconfined compression) or a spherical impermeable indenter with a radius of 1.53 mm (indentation). After full relaxation, an additional 5% strain at a ramp strain rate of 0.001 s^{-1} was applied. This strain was held constant until full relaxation. While the additional 5% straining and relaxation occurred, axial reaction forces were computed. The used samples were taken from the patellae of mature 1–2-year-old cattle.

Results

DETERMINATION OF UNKNOWN MATERIAL PROPERTIES

The depth-dependent permeability of the model [Eq. (12)] was fitted to experimental data of Maroudas[17] (Fig. 2). The resulting value for M was 1.339.

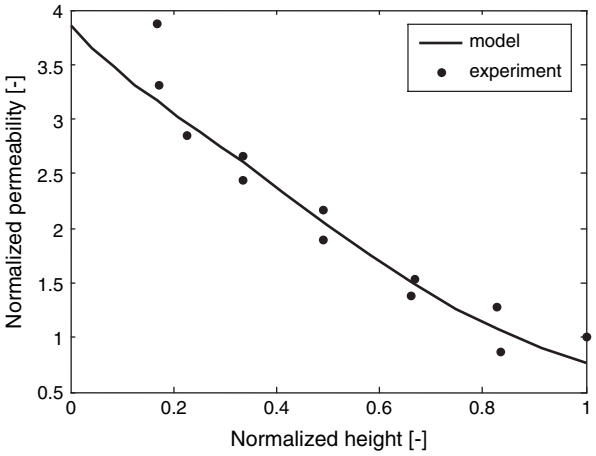

Fig. 2. Depth-dependent permeability as measured by Maroudas *et al.* (1976) along with the FEA-model curve fit.

The fit of the model to the 1D-swelling data of Eisenberg and Grodzinsky[25] resulted in a value for G_m of 0.903 MPa. The normalized reaction force was almost in perfect agreement with the experimental data [Fig. 3(a)].

The remaining unknown material parameters E_1, E_2, k_1, k_2, η_0 and α were determined by fitting the confined compression, unconfined compression and indentation data of DiSilvestro and Suh[24], and 1D-swelling data of Wilson *et al.*[4] (Figs. 3(b)–6). The resulting model parameters were determined at $E_1 = 4.316$ MPa, $E_2 = 19.97$ MPa, $k_1 = 16.85$, $k_2 = 41.49$, $\eta = 1.424 \times 10^5$ MPa s and $\alpha = 1.767 \times 10^{-17}$ m^4/N s.

All model fits were in good agreement with the experimental data. The coefficients of determination (R^2) for the different fits are given in Table I.

Discussion

The goal of this study was to develop a model for articular cartilage in which all local material properties are the direct consequence of the local composition of the tissue. Such a model enables us to study the influence of local changes in composition that occur during cartilage degeneration and adaptation. To do this our fibril-reinforced poroviscoelastic swelling model for articular cartilage[26] was combined with our tissue composition-based model[4], and expanded with a new permeability law and a new law for the viscoelastic behavior of the collagen network. The new permeability law is based on the assumption that both the depth- and strain-dependencies of the permeability are governed by the same mechanism and are the direct result of the composition of the tissue. We have previously shown that this model can account for the strain-dependent compressive equilibrium properties of articular cartilage during confined compression[4]. In the current study it has been shown that this model can also account for the transient behavior of articular cartilage. It was shown that the combined model can simultaneously describe the behavior of articular cartilage in confined compression, unconfined compression, indentation and two different 1D-swelling tests. With the proposed permeability law, the strain-dependent permeability of articular cartilage can be explained. There is no literature data available to compare directly to the strain-dependent permeability.

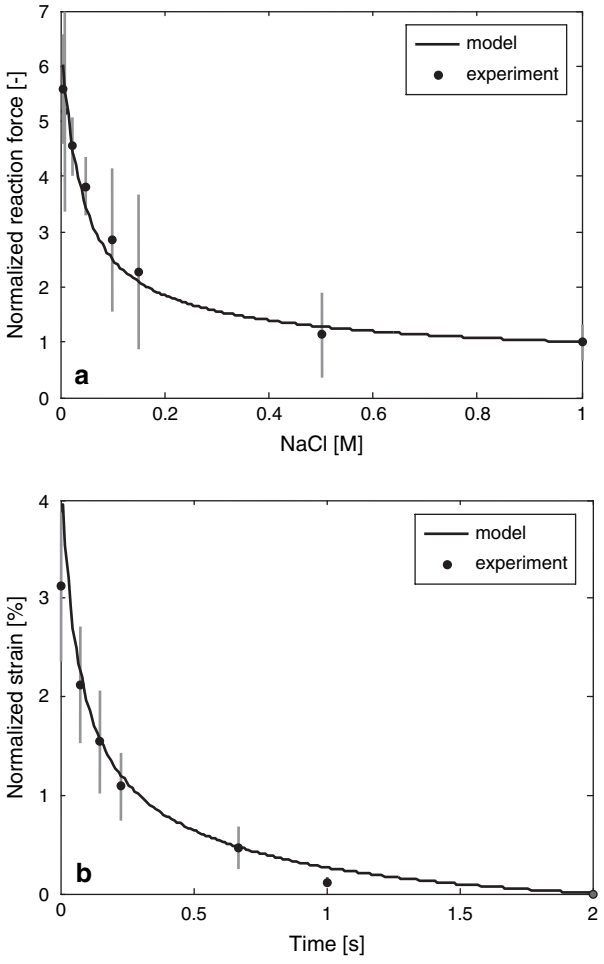

Fig. 3. (a) Axial reaction force, normalized with the reaction force at an external salt concentration of 2 M, measured from 1D swelling tests (Eisenberg and Grodzinsky, 1985) along with FEA-model curve fit. (b) Axial strain measured from 1D free swelling tests (Wilson *et al.*, 2005c) along with FEA-model curve fit.

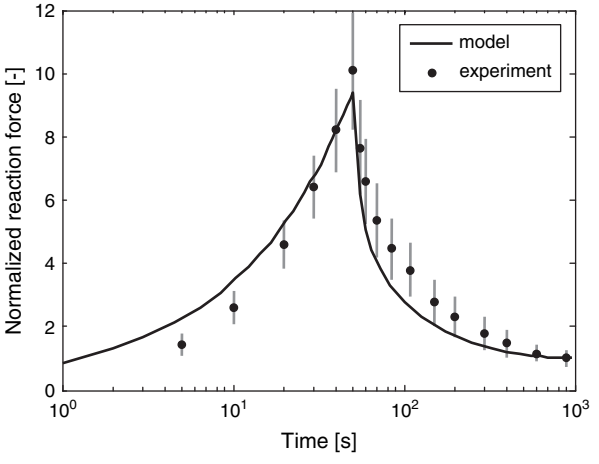

Fig. 4. Axial reaction force, normalized to equilibrium, measured from confined compression tests[24] along with FEA-model curve fit.

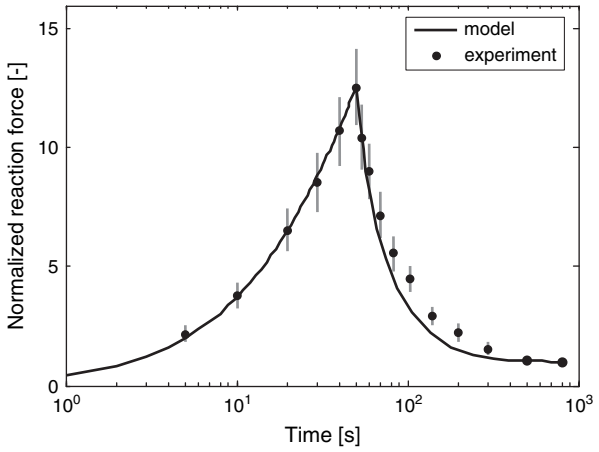

Fig. 5. Axial reaction force, normalized to equilibrium, measured from indentation tests[24] along with FEA-model curve fit.

However, since the resulting strain- and time-dependent behavior of the model concur with the experimental data, it is concluded that the strain-dependent permeability in the model is correct.

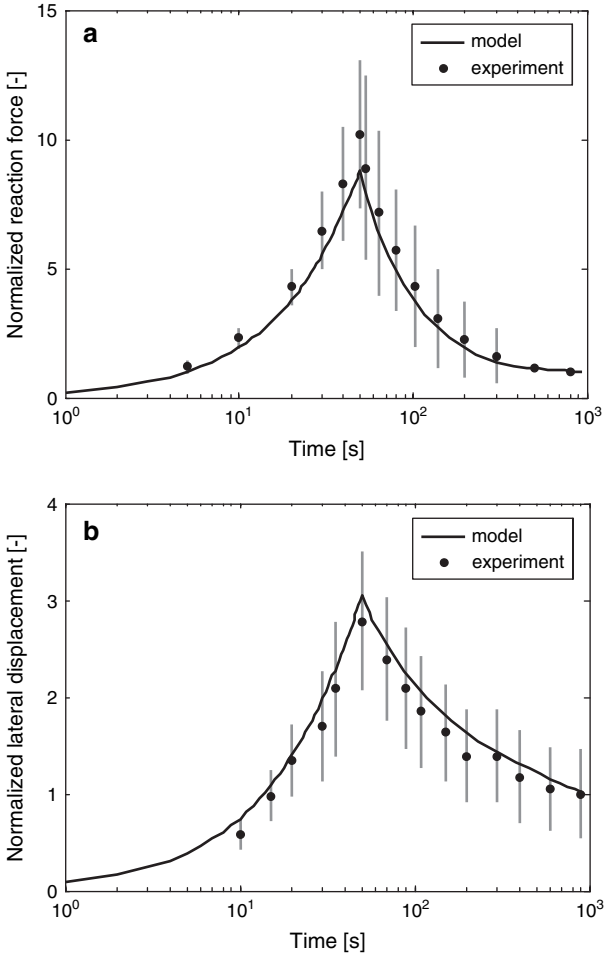

Fig. 6. (a) Axial reaction force, normalized to equilibrium, measured from unconfined compression tests[24] along with fibril-reinforced model curve fit. (b) Lateral displacement, measured from unconfined compression tests[24] along with FEA-model curve fit.

Table I
The coefficients of determination (R^2) for the performed model fits

Test	R^2
Permeability[17]	0.930
1D-swelling confined swelling[25]	0.977
1D-swelling free swelling[4]	0.980
Confined compression[24]	0.938
Unconfined compression (reaction force)[24]	0.998
Unconfined compression (lateral displacement)[24]	0.987
Indentation[24]	0.985

All material parameters (G_m, E_1, E_2, k_1, k_2, η_0, α and M) were assumed constant over the depth of the tissue and were derived from fits to experimental data. Hence, all depth-dependent behavior is due to the depth-dependent tissue composition and structure. As the tissue composition was not measured in experiments that were used to fit our material parameters, we were obliged to base the prescribed tissue composition on distinct literature data. Due to this there might be an error in the obtained material parameters.

Viscoelastic and anisotropic properties of the biphasic nonfibrillar matrix[5] were not included in this model. Although we anticipate that the major viscoelastic and anisotropic properties of the solid matrix come to the account of the fibrillar part, this may also explain part of the mismatches between the model and the experimental data.

As we used a biphasic swelling model the influence of ion fluxes on the transient behavior of articular cartilage have not been included in this study. However, as it was shown in Wilson *et al.*[33] that under physiological conditions the biphasic swelling model behaves very similar to the full mechano-electrochemical model, it is assumed that this does not significantly influence our results.

To the best of our knowledge this is the first model that includes a continuous depth-dependent permeability that is based on the tissue composition, with constant, not depth-dependent mechanical properties of the tissue components themselves. Previously, depth-dependent permeability was included by directly defining different permeability values for different layers of the tissue[38,39].

In conclusion, our recently developed composition-based cartilage model[4] was expanded with a new permeability law and a new law for the viscoelastic behavior of the collagen network of articular cartilage. In the new permeability law the permeability is only dependent on the extra-fibrillar fluid fraction. With this law both the depth- and strain-dependent permeabilities of articular cartilage can be explained based on the composition of the tissue, with constant material properties for the tissue constituents themselves. In the resulting model all local material properties are the direct consequence of the local composition and structure of the tissue. This new model will enable us to study the influence of well-characterized local changes in composition that can occur during cartilage degeneration and adaptation.

Acknowledgments

This project was supported by a grant from the AO Foundation, Switzerland.

Appendix A. Determination of the viscoelastic fibril stress

The stresses in the dashpot and the spring S_2 in Fig. 1 must be the same. Hence, P_2 can also be given by

$$P_2 = \eta\dot{\varepsilon}_v = \eta(\dot{\varepsilon}_f - \dot{\varepsilon}_e), \tag{A1}$$

where ε_v is the dashpot strain, and η the dashpot constant. From Eq. (4) follows that

$$\varepsilon_e = \frac{1}{k_2}\log\left(\frac{P_2}{E_2}+1\right), \quad \dot{\varepsilon}_e = \frac{\dot{P}_2}{(P_2+E_2)k_2}. \tag{A2}$$

The time derivative of the fibril strain is then given by

$$\dot{\varepsilon}_f = \dot{\varepsilon}_e + \dot{\varepsilon}_v = \frac{\dot{P}_2}{(P_2+E_2)k_2} + \frac{P_2}{\eta}. \tag{A3}$$

From Eqs. (A1) and (A3), and after time integration with an implicit backward Euler scheme, P_2 becomes

$$\begin{aligned} P_2 &= -\frac{b}{2} + \frac{1}{2}\sqrt{b^2-4c} \quad \text{for } \varepsilon_e > 0 \\ P_2 &= 0 \qquad\qquad\qquad\quad \text{for } \varepsilon_e \le 0 \end{aligned}, \tag{A4}$$

with

$$b = -\frac{\varepsilon_f^{t+\Delta t} - \varepsilon_f^t}{\Delta t}\eta + \frac{\eta}{k_2\Delta t} + E_2, \tag{A5}$$

$$c = -\frac{\varepsilon_f^{t+\Delta t} - \varepsilon_f^t}{\Delta t}\eta E_2 - \frac{\eta P_2^t}{k_2\Delta t}. \tag{A6}$$

References

1. Atkinson RS, Haut RC, Altiero NJ. An investigation of biphasic failure criteria for impact-induced fissuring of articular cartilage. J Biomech Eng 1998;120(4):536–7.
2. Morel V, Quinn TM. Cartilage injury by ramp compression near the gel diffusion rate. J Orthop Res 2004; 22(1):145–51.
3. Wilson W, Burken CG, van Donkelaar CC, Buma P, van Rietbergen B, Huiskes R. Causes of mechanically induced collagen damage in articular cartilage. J Orthop Res (in press).
4. Wilson W, Huyghe JM, van Donkelaar CC. Depth-dependent compressive equilibrium properties of articular cartilage explained by its composition. Biomech Model Mechanobiol (in press).
5. Mak AF. The apparent viscoelastic behavior of articular cartilage – the contributions from the intrinsic matrix viscoelasticity and interstitial fluid flows. J Biomech Eng 1986;108(2):123–30.
6. Mak AF. Unconfined compression of hydrated viscoelastic tissues: a biphasic poroviscoelastic analysis. Biorheology 1986;23(4):371–83.
7. Suh JK, Bai S. Finite element formulation of biphasic poroviscoelastic model for articular cartilage. J Biomech Eng 1998;120(2):195–201.
8. Maroudas A. Physicochemical properties of articular cartilage. In: Freeman MAR, Ed. Adult Articular Cartilage. 2nd edn. Kent, UK: Pitman Med 1979:215–223.
9. Mow VC, Ratcliffe A. Structure and function of articular cartilage and meniscus. In: Mow VC, Hayes WC, Eds. Basic Orthopaedic Biomechanics. 2nd edn. Philadelphia: Lippincott-Raven 1997:113–177.
10. Gu WY, Lai WM, Mow VC. Transport of fluid and ions through a porous-permeable charged-hydrated tissue, and streaming potential data on normal bovine articular cartilage. J Biomech 1993;26:709–23.
11. Gu WY, Lai WM, Mow VC. A mixture theory for charged-hydrated soft tissues containing multi-electrolytes: passive transport and swelling behaviors. J Biomech Eng 1998;120:169–80.
12. Maroudas A. Transport of solutes through cartilage: permeability to large molecules. J Anat 1976;122:335–47.
13. Lai WM, Mow VC. Drag-induced compression of articular cartilage during a permeation experiment. Biorheology 1980;17:111–23.
14. Mow VC, Kuei SC, Lai WM, Armstrong CG. Biphasic creep and stress relaxation of articular cartilage in compression: theory and experiments. J Biomech Eng 1980;102:73–84.
15. Gu WY, Yao H. Effects of hydration and fixed charge density on fluid in charged hydrated soft tissues. Ann Biomed Eng 2003;31:1162–70.
16. Maroudas A. Physicochemical properties of cartilage in the light of ion exchange theory. Biophys J 1968;8: 575–95.
17. Maroudas A. Biophysical chemistry of cartilaginous tissues with special reference to solute and fluid transport. Biorheology 1975;12:233–48.
18. Holmes MH, Mow VC. The nonlinear characteristics of soft gels and hydrated connective tissues in ultrafiltration. J Biomech 1990;23:1145–56.
19. Gu WY, Yao H, Huang CY, Cheung HS. New insight into deformation-dependent hydraulic permeability of gels and cartilage, and dynamic behavior of agarose gels in confined compression. J Biomech 2003;36:593–8.
20. Urban JPG, McMullin JF. Swelling pressures of the lumbar intervertebral discs: influence of age, spinal level, composition and degeneration. Spine 1988;13: 179–87.
21. Maroudas A, Bannon C. Measurement of swelling pressure in cartilage and comparison with the osmotic pressure of constituent proteoglycans. Biorheology 1981;18:619–32.
22. Katz EP, Wachtel EJ, Maroudas A. Extra-fibrillar proteoglycans osmotically regulate the molecular packing of collagen in cartilage. Biochim Biophys Acta 1986; 882:136–9.
23. Maroudas A, Wachtel E, Grushko G, Katz EP, Weinberg P. The effect of osmotic and mechanical pressures on water partitioning in articular cartilage. Biochim Biophys Acta 1991;1073:285–94.
24. DiSilvestro MR, Suh JK. A cross-validation of the biphasic poroviscoelastic model of articular cartilage in unconfined compression, indentation, and confined compression. J Biomech 2001;34:519–25.
25. Eisenberg SR, Grodzinsky AJ. The kinetics of chemically induced nonequilibrium swelling of articular cartilage and corneal stroma. J Biomech Eng 1987;109: 79–89.
26. Wilson W, van Donkelaar CC, van Rietbergen B, Huiskes R. A fibril-reinforced poroviscoelastic swelling (FPVES) model for articular cartilage. J Biomech 2005;38:1195–204.
27. Charlebois M, McKee MD, Buschmann MD. Nonlinear tensile properties of bovine articular cartilage and their variation with age and depth. J Biomech Eng 2004; 126:129–37.

28. Fung YC. Mechanical Properties of Living Tissues. New York: Springer Verlag 1981.
29. Morgan FR. The mechanical properties of collagen fibers: stress–strain curves. J Soc Leather Trades Chem 1960;44:171–82.
30. Roth V, Mow VC. The intrinsic tensile behavior of the matrix of bovine articular cartilage and its variation with age. J Bone Joint Surg Am 1980;62: 1102–17.
31. Woo SL, Simon BR, Kuei SC, Akeson WH. Quasi-linear viscoelastic properties of normal articular cartilage. J Biomech Eng 1980;102:85–90.
32. Wilson W, van Donkelaar CC, van Rietbergen C, Ito K, Huiskes R. Stresses in the local collagen network of articular cartilage: a poroviscoelastic fibril-reinforced finite element study. J Biomech 2004;37:357–66.
33. Wilson W, van Donkelaar CC, Huyghe JM. A comparison between mechano-electrochemical and biphasic swelling theories for soft hydrated tissues. J Biomech Eng 2005;127:158–65.
34. Lanir Y. Biorheology and fluid flux in swelling tissues. I. Bicomponent theory for small deformations, including concentration effects. Biorheology 1987;24:173–87.
35. Huyghe JM, Houben GB, Drost MR, van Donkelaar CC. An ionised/non-ionised dual porosity model of intervertebral disc tissue. Biomech Model Mechanobiol 2003; 2:3–19.
36. van der Voet A. A comparison of finite element codes for the solution of biphasic poroelastic problems. Proc Inst Mech Eng [H] 1997;211:209–11.
38. Chen SS, Falcovitz YH, Schneiderman R, Maroudas A, Sah RL. Depth-dependent compressive properties of normal aged human femoral head articular cartilage: relationship to fixed charge density. Osteoarthritis Cartilage 2001;9:561–9.
39. Krishnan RS, Park S, Eckstein F, Ateshian GA. Inhomogeneous cartilage properties enhance superficial interstitial fluid support and frictional properties, but do not provide a homogeneous state of stress. J Biomech Eng 2003;125:569–77.